Journal of Materials Chemistry C

Accepted Manuscript

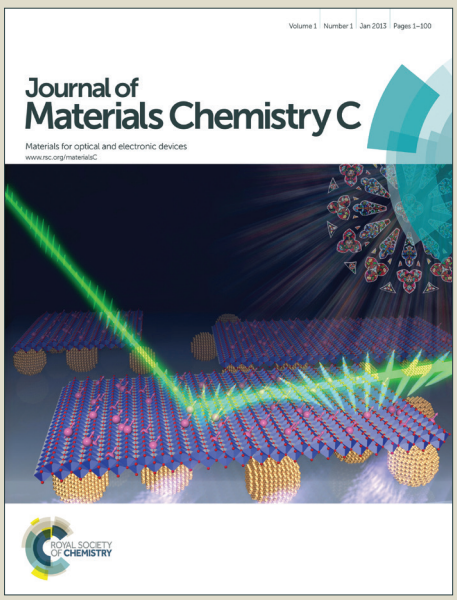

ROYAL SOCIETY OF CHEMISTRY

www.rsc.org/materialsC

Efficient Multicolor and White Light Emission From Zr-Based MOF Composites: Spectral and Dynamical Properties

Mario Gutiérrez,[1] Félix Sánchez[2] and Abderrazzak Douhal[1]*

[1]Departamento de Química Física, Facultad de Ciencias Ambientales y Bioquímica, INAMOL, Universidad de Castilla-La Mancha, Avenida Carlos III, S.N., 45071 Toledo, Spain.

[2] Instituto de Química Orgánica, CSIC, Juan de la Cierva, 3, 28006 Madrid, Spain.

*Corresponding author at Universidad de Castilla-La Mancha.

Tel.: +34 925 265 717; E-mail address: abderrazzak.douhal@uclm.es

Abstract

We report on the spectroscopy and dynamics of a Zr-naphthalene dicarboxylic acid (Zr-NDC) MOF interacting with three laser dyes: Coumarin 153 (C153), Nile Red (NR) and 4-(dicyanomethylene)-2-methyl-6-(4-dimethylaminostyryl)-4H-pyran (DCM) in diethyl ether (DE) suspensions. The photoexcitation of the MOF forming the composites (dyes@MOF) leads to an energy transfer (ET) to the trapped dyes, opening the door to tune the materials emission. Trapped C153 molecules exhibit two different ET dynamics. At lower C153 concentrations, the mean ET time process (from MOF monomers) is in ~3.3 ns, whereas at higher ones it is in ~360 ps. These mean ET times, which are guest-concentration dependent, reflect the different dye occupancies into the MOF pores. For trapped NR and DCM molecules, because of a different emission (energy donor) and absorption (energy acceptor) spectral overlap, the ET takes place from the excimers and not from the monomers. Solvent suspensions of Zr-NDC MOF trapping these three dyes show a multicolor, and white light emission, having quantum yields up to 41 %. More specifically, NR/C153@Zr-NDC in diethyl ether suspension gives three emission bands having their intensity maxima at ~385, ~500 and ~660 nm. This combination produces a white light, having CIE coordinates (0.32, 0.34) very near to the ideal ones (0.33, 0.33). Our findings open the door to develop fluorescence nanomaterial sensors and white light LEDs based on Zr-NDC MOF.

1. Introduction

Metal-Organic Frameworks (MOFs) have become one of the most promising materials for a wide range of uses and applications.[1, 2] Among them, the implementation of MOFs as fluorescent chemical sensors and light emitting devices has raised a great interest in the scientific community.[3-5] As a result, a great number of luminescent MOFs has been employed to sense different chemical compounds like explosives,[6-8] volatile organic molecules (VOMs)[9, 10] or cations.[11-13] Others have been designed to emit white light for developing white light emitting devices (WLEDs).[14, 15] WLEDs have been also fabricated by coating a blue light emitting diode (LED) with highly luminescent MOFs yellow phosphor based on $Zn_6(btc)_4(tppe)_2(DMA)_2$ or $Zn_2(tcbpe)_xDMA$.[16, 17] For both MOFs, the immobilization of the organic linkers by its incorporation into the network leads to an increase in the internal as well as external quantum yields, improving their photoluminescence properties, like luminescent and moisture stability and color tunability. Moreover, one of the most favorable morphological characteristics of MOFs is their porous structure, which permits the inclusion of different guests.[18, 19] The formed host-guests composites materials can exhibit different photoevents processes as charge- and energy-transfer (CT, ET). [20, 21] For example, an efficient ET was observed by incorporating an europium β-diketonate complex into the porous matrix of HKUST-1 MOF, making the material a photoantennae enhancing the emission of the lanthanide complex.[22] Others excited MOFs show ET to laser dyes (4-(dicyanomethylene)-2-methyl-6-(4-dimethylaminostyryl)-4H-pyran (DCM) and Rhodamine B (Rho B)), leading to a dual emission, which was used to detect volatile organic compounds (VOCs).[23, 24] Zn(OPE) MOF experiences a large decrease in its emission intensity giving birth to a red-shifted emission band of trans-4-[4-(dimethylamino)styryl]-1-methylpyridinium iodide (DSMP) dye due to an ET process.[25] MOF-177 trapping α,ω-dihexylsexithiophene (DH6T) and [6,6]-phenyl-C61-butyric acid methyl ester (PCBM) shows a cascaded MOF-177→DH6T→PCBM ET, paving the wave to use in organic photovoltaics.[26] Recently, a white light emitting device (WLED) was developed by incorporating a cationic Ir^{III} complex into the porous structure of a Cd-based MOF.[27] An In-based MOFs containing pyridine hemicyanine and acridine dyes have been also reported to display white light emission opening the possibility to their use as WLED.[28]

From the point of view of dynamics, only few studies on the transfer of energy between the MOF and guests molecules have been reported.[29, 30] QD550 and QD620 quantum dots transfer their energies to porphyrin-based MOF (F-MOF and DA-MOF) which take place in 1.7 and 4.1 ns from QD550, and 9.6 and 2.1 ns from QD660, to F-MOF and DA-MOF,

respectively.[29] Shorter ET events (9 ps) have been recorded from trapped bisanthracene to a Pd-based MOF.[30] Time-resolved studies can shed light on the photophysical processes that govern the photonics and photosensing of these hybrid materials, and indeed, ultrafast spectroscopy will unravel the key mechanisms of these photobehaviours,[31] which will allow a better design of novel fluorescent based-MOFs composites for photonic applications.

Herein, we report on the spectroscopic and dynamical properties of host-guest composites materials of a Zr-based MOF (Zr-NDC) interacting with three laser dyes: Coumarin 153 (C153), Nile Red (NR) and (4-(dicyanomethylene)-2-methyl-6-(4-dimethylaminostyryl)-4H-pyran (DCM). By trapping these dyes into the Zr-NDC porous structure, we could tune the emission of the composite material due to ET photoevents. For example, incorporating Coumarin 153 (C153) or Nile Red (NR), we could modulate the emission from blue (MOF) to green (C153) or red (NR). Interestingly, we obtained white light emitting composite materials by simultaneously incorporating C153 and NR, or (4-(dicyanomethylene)-2-methyl-6-(4-dimethylaminostyryl)-4H-pyran (DCM), giving high fluorescence quantum yields (up to 41%). The obtained white light is of a good quality as shown by the International Commission on Illumination (CIE) coordinates (0.32, 0.34) and (0.32, 0.31), which are very close to that of the ideal ones (0.33, 0.33). From a dynamics point of view, the mean ET time processes from MOF to trapped dyes of the composite materials (MOF containing C153, NR or DCM) were obtained. Our results show that C153 molecules are trapped within two different pores of the MOF in which the mean ET time (from MOF monomers) changes from 3.3 ns to 360 ps. However, NR and DCM molecules are too large to be included into the tetrahedral (smaller) pores, and only the octahedral ones could be filled. For both composites, and contrary to the observed for C153@MOF one, the energy is transferred from MOF excimers to these dyes. Our findings open the possibility of Zr-NDC MOFs containing dyes to potential applications in diverse fields of science and technology like fluorescent nanosensors and WLEDs.[32]

2. Experimental Section

Zr-NDC was prepared according to the procedures reported in the original references.[33, 34] Briefly, $ZrCl_4$ (0.4 g, 1.7 mmol) in dimethylformamide (DMF) (75 mL) was dispersed by ultrasound at 50-60 °C and then acetic acid (2.85 mL, 850 mmol) was added. A DMF solution (25 mL) of the 2,6-naphthalene dicarboxylic acid (368 mg, 1,7 mmol) linker was added to the above solution in an equimolar ratio with regard to $ZrCl_4$. Finally, water (0.125 mL, 0.007 mmol) was added to the solution. The tightly capped flask was sonicated at

60 °C and kept in a bath at 120 °C under static conditions during 24 h. After 24 h, the solutions were cooled to room temperature and the precipitate was isolated by centrifugation. The solid was washed with DMF (10 mL). After standing at room temperature for 2 h, the suspension was centrifuged and the solvent was decanted off. The obtained particles were washed several times with ethanol. Finally, the solid was dried under reduced pressure (80 °C, 3 h). X-ray diffraction (Bruker D8 diffractometer, Cu Kα radiation) was used to confirm the crystalline structure of the Zr-NDC.

2.1. Synthesis of dye@Zr-NDC Composite Materials

For the spectroscopic studies, the solvent (anhydrous) diethyl ether (DE, 99.9%) was from Sigma-Aldrich, and used as received. To prepare the host-guest complex C153@Zr-NDC, different aliquots of C153 in a diethyl ether (DE) solution were added to 20 mL of DE containing 20 mg of Zr-NDC. After sonicating during 15 min, the mixture was washed several times and the yellow C153@Zr-NDC solid was collected using a fresh diethyl ether solution. The loading (calculated using the C153 UV-visible absorption spectrum before and after its interaction with MOF) at the C153 maximum concentration ($1x10^{-4}$ M) was 90 %. The amount of trapped C153 was 27.5 μg C153 / mg MOF. We do not observe any change in the absorption nor emission spectra of C153@Zr-NDC in a DE suspension after 24 hours of sample preparation. Similar procedure was followed to prepare NR@Zr-NDC and DCM@Zr-NDC. For these cases, NR and DCM in DE solutions were added to a 10 mg/10 ml Zr-NDC DE suspension to have a final dye concentration of $2.5x10^{-5}$ and $1.5x10^{-5}$ M, respectively. The resulted mixtures were washed and collected using fresh ether ethylic suspensions. The loading of NR is 60% while that of DCM is 80%, both of them calculated in similar way than that of C153. The amounts of trapped NR and DCM are 4.7 μg NR / mg MOF and 3.6 μg DCM / mg MOF. Both samples in DE suspensions were stable up to 5 hours showing no changes in the absorption and emission spectra. Longer times induce a partial release of these dyes from the MOF.

The multiguest system NR/C153@Zr-NDC was prepared by adding NR in DE solution (with a dye concentration of $5x10^{-6}$ M) to a 10 mg/10 ml Zr-NDC DE suspension. After sonicating during 15 minutes, a C153 DE solution was added to the NR@Zr-NDC DE suspension (having a final C153 concentration of $3x10^{-6}$ M), sonicating again during 15 min. The mixture was washed and collected using fresh DE solvent. The solvent suspensions were prepared by adding ~1 mg of dyes@Zr-NDC solid to ~20 mL of the solvent and sonicating during 5 minutes.

2.2. Structural, Spectroscopic and Dynamical Measurements

The MOF and dyes@MOF X-ray diffraction traces of a polycrystalline powder were performed using a PANalytical® diffractometer, X´Pert Pro model as polycrystalline powder. The conditions used were: 45 Kv, 40 mA, CuKα radiation and a system of slits (soller – mask– divergence – antiscatter) of 0.04 rad - 10 mm - 1/8º - 1/4º with a X´celerator detector. The results (Figure S1 in ESI†) indicate that the crystallinity and morphology of the composite materials are not different from those of the MOF powder.

The steady-state UV-visible absorption and fluorescence spectra measurements were carried out using JASCO V-670 and FluoroMax-4 (Jobin-Yvone) spectrophotometers, respectively. The fluorescence quantum yields of the host-guest complexes dyes@Zr-NDC DE suspensions were measured using an integrating sphere setup Quanta from Horiba coupled to FluoroMax-4 (Jobin-Yvone) spectrophotometer. The picosecond time-resolved emission experiments have been recorded employing a time-correlated single-photon counting (TSCPC) system.[35] The samples were excited by a 40 ps-pulsed (<1 mW, 40 MHz repetition rate) diode-laser (PicoQuant) centred at 370, 433 and 635 nm respectively. The instrument response function (IRF) of each diode-laser is around ~70 ps. The fluorescence signal was gated at magic angle (54.7°), and monitored at a 90° angle to the excitation beam at discrete emission wavelengths. The decays were deconvoluted and fitted to a multiexponential function using the FLUOFIT package (PicoQuant) allowing single and global fits. The quality of the fits as well as the number of exponentials were carefully selected based on the reduced $\chi 2$ values (which were always below <1.2) and the distributions of the residuals. All the experiments were done at room temperature (295 K).

3. Results and Discussion

As said in the Introduction part, excited MOFs-based systems have been reported to show energy transfer (ET) to trapped molecules like 4-(dicyanomethylene)-2-methyl-6-(4-dimethylaminostyryl)-4H-pyran (DCM),[23] Rhodamine B,[24] dihexylsexithiophene (DH6T)[26] or bisanthracene.[30] They also can act as energy acceptors from other systems like quantum dots.[29] Here, we examined the possibility of an ET processes from a Zr-based MOF to different fluorescent dyes. We selected Zr-NDC MOF due to its intense blue light emission

which can overlap with the absorption of these fluorescent dyes, and owing to its porous structure which is composed of two different internal cavities (a octahedral central cage with a pore size of ~14 Å surrounded by eight corner tetrahedral ones whose pores size is ~11 Å)[36] where it is possible to allocate guests having appropriate sizes. A previous report demonstrated that the Zr-NDC blue emission in diethyl ether (DE) suspension is originated by a combination of monomers and excimers fluorescence.[37] The excimers formation takes place in 650 ps, whereas the monomers and excimers lifetimes are 3.7 and 13.9 ns, respectively.

To explore the ligand-guest interactions, we performed steady-state and ps-ns time-resolved emission studies of Zr-NDC interacting with C153, NR and DCM in DE suspensions. We also studied the complexes formed by Zr-NDC containing both C153 and NR.

3.1. Coumarin153@Zr-NDC Composite

To begin with, we investigated the possibility to tune the emission color of the formed hybrid materials by trapping C153 into the MOF cages. We select C153 due to its highly fluorescence intensity and small size (Scheme S1 in Supporting Information) which could be incorporated into both the tetrahedral and octahedral cavities of the MOF, and its strong absorption in the Zr-NDC emission region, which can favor an ET process from the excited MOF.

3.1.1. Steady-State UV-Visible Absorption and Emission Spectra

We have successfully trapped C153 within Zr-NDC in DE suspensions by simply sonicating the mixture (using [C153] = $1x10^{-4}$ M we got a loading of 90%). Figure 1 shows a comparison of the UV-visible absorption and emission spectra between Zr-NDC, C153 and the C153@Zr-NDC hybrid material in DE. While the C153@Zr-NDC absorption spectrum reproduce those of MOF and C153 in DE (Figure 1A), that of fluorescence shows a strong decrease in the emission intensity of Zr-NDC, and an increase in the C153 one, with a large red shift (~30 nm, 1250 cm^{-1}) when comparing with the emission of a C153 in a DE solution (Figure 1B). Firstly, the red shift indicates a change in the environment of trapped C153 which reflects a strong interaction with Zr-NDC, similar to a previous observation for which C153 was incorporated into silica nanochannels.[38] Secondly, a large decrease in the MOFs naphthalene monomers emission intensity also reflects a strong interaction with C153. Comparable quenching of the MOF emission intensity was described for DH6T@MOF-177

and assigned to an ET process.[26] As the shape of the emission spectrum does not change after washing with DE several times the hybrid material, we conclude that C153 molecules are trapped within the cages of the MOF. Based on the maxima of the absorption and emission spectra of trapped C153, we suggest that the polarity into the MOF cavities must be similar to that of DO.[39] The fluorescence quantum yield (φ) of C153@Zr-NDC exciting at 335 nm is φ = 0.41±0.03.

To examine the possibility of ET from the MOF naphthalene ligands to the trapped C153, we first looked at the excitation spectra of the complex in DE and gating at the C153 emission (625 nm), where the MOF does not emit. The spectrum (inset in Figure 1A) clearly reproduces the absorption bands of Zr-NDC together with the C153 one (but having a different relative intensity ratio), indicating the occurrence of an ET process from the excited MOF to the encapsulated dye. Note also that the spectral position of C153 emission does not change with the excitation wavelength (from 335 to 410 nm). Exciting at 335 nm we observed the MOF emission bands (~390 nm) and that of the trapped C153 molecules, having its maximum intensity at 505 nm. Moreover, exciting the C153@Zr-NDC composite at 410 nm, the emission band corresponding to C153 molecules is also red-shifted (505 nm), reflecting that these molecules have the same environment (trapped into MOF) as those receiving energy from the excited MOF. To get information on the maximum loading of Zr-NDC with C153 and the possibility of tuning the emission from blue to green light (see the inserted pictures in Figure 1B), different amounts of C153 were added to a Zr-NDC DE suspension. Figure 2 A shows the changes in the emission spectrum of the formed complexes with different additions of C153. At lower C153 concentrations, the emission spectra are similar to that obtained for pure Zr-NDC, however when the concentration of C153 increases, the Zr-NDC emission begins to drop while that of C153 grows up. Analogous behavior was observed for Rho@CZJ-3 which exhibits a decrease in the emission intensity ratio upon increasing the dye concentration allocated into the MOF.[24] To analyze the changes, Figure S2 (ESI†) exhibits a plot of the emission intensities ratio ($I_{(C153)}/I_{(Zr\text{-}NDC)}$) vs C153 concentration, where we see a linear behavior indicating that almost all the added C153 is interacting with the MOF. We then calculated the loading (using the C153 absorption spectra before and after its interaction with MOF) of the C153 within the MOF and found 90 % at most higher concentration ($1x10^{-4}$ M).

3.1.2. Picosecond-Time Resolved Emission Study

To explore the dynamical behavior of energy transfer from Zr-NDC to the trapped C153 molecules, we studied the emission decays of the complexes in DE suspensions, exciting at 371 and 433 nm and observing at different wavelengths. Figures S3 A,B (ESI†) show a comparison of the decays of Zr-NDC and C153@Zr-NDC complex in DE suspensions, observing at 425 and 525 or 550 nm, respectively. At these wavelengths, we mainly observe the signal from the monomers (425 nm), excimers (525 nm) and trapped C153 molecules (550 nm). Table 1 gives the obtained time constants values exciting at 433 and 371 nm, respectively. Exciting at 433 nm (only the C153 absorbs), the fluorescence decays of free C153 in a DE solution are monoexponential functions, giving a lifetime of 5.4 ns, while those of trapped C153 molecules behave as biexponential decays giving short (1.9 ns) and long (6.9 ns) components (Table 1A), reflecting the heterogeneity of the surrounding medium. In addition to the existence of two different (in shape and volume) pores, this MOF can have defects on ligands and nodes contents, leading to different effect on the photophysical properties of the dye.

Exciting at 371 nm (Zr-NDC absorption region) and gating the emission at the blue part (400-435 nm), C153@Zr-NDC exhibits a multiexponential behavior giving three decaying components of τ_1= 360 ps, τ_2= 2.5 ns and τ_3= 6.8 ns; while at the green-red region (475-600 nm), where the fluorescence is mainly from trapped C153, we found a rising component of 360 ps, and decaying one of 6.8 ns (Table 1B). This latter (having its maximum contribution at the green-red part) is due to the trapped C153 decay as it is not very different from that obtained (6.9 ns) when exciting at 433 nm (Table 1A), where only the trapped C153 absorbs. At this wavelength the MOF cannot be excited. The increase in the lifetime of the trapped C153 molecules (6.8 ns) compared to the free ones (5.4 ns) reflects the hydrophobicity nature of the MOF cavities. It has been described that the lifetime when C153 molecules are trapped into the hydrophobic sites of poly(N-vinylcarbazole) (PVK) nanoparticles changes from ~1 ns (water solution) to ~5 ns.[40] On the other hand, the 2.5 ns component, having its maximum contribution at the blue part, is due to the decay of the Zr-NDC monomers. Note the decrease (from 3.7 to 2.5 ns) in the MOF lifetime values when compared to that observed for Zr-NDC monomers without C153.[37] Finally, the 360 ps component, decaying at the blue region and rising at the red one, is the signature of an ET process from excited Zr-NDC to trapped C153 molecules. The lack of MOF excimers lifetime together with the decrease in the monomer lifetimes suggest that the included C153 does not allow MOF excimers formation. This leads to an ET from the monomers to C153 in 360 ps, a value shorter than that of excimers formation (650 ps) without C153. Moreover, the shortest component (1.9 ns) observed when excited at 433 nm is not present when exciting at Zr-NDC

absorption region (371 nm), indicating that these populations of trapped C153 are not receiving energy from the excited MOF. We suggest that they are not in the right orientation/position to receive energy from the naphthalene linkers.

Moreover, because of the possibility of C153 to be included in different pores of Zr-NDC, we examined the site-specific energy transfer within the complexes. To this aim, we examined the emission risetime of the trapped C153 using different amounts of it. Figure 2 B shows representative signals of the emission rise and decay observed at 550 nm and exciting the C153@Zr-NDC complexes at 371 nm. Table 2 gives the values of the risetimes at each C153 concentration, and Figure 2C illustrates the results. We can distinguish three C153-concentration dependent behaviors of the rising component: I) at low added [C153] ($<0.05x10^{-4}$ M), we observed an increase in the risetime value (reaching its maximum τ = 3.3 ns at 1.25 x 10^{-6} M;). II) When the [C153] increases (up to $0.2x10^{-4}$ M), the recorded risetime value decreases abruptly, and III) for added [C153] ($>0.2x10^{-4}$ M) the risetime does not show too much change (from 0.7 to 0.36 ns). To discuss the above observations, we focus on the longest (τ_L ~3.3 ns) and shortest (τ_S ~0.36 ns) rise-times as they reflect the limit of the observed mean time ET dynamics under the used experimental conditions. As ET rate depends on the acceptor-donor distance and orientations, at lower concentrations of C153 (acceptor) the mean ET time is longer, indicating that the distance and orientation of the donor-acceptor pair is not favoring the ET process. However at higher C153 concentrations, the mean ET time is shorter reflecting a closer distance and/or better orientations between the involved moieties. Based on these results, we suggest that at lower C153 concentrations, the dye is mainly trapped into the octahedral pores which are larger, allowing relatively longer the distance between the naphthalene ligands and C153 molecules. Increasing C153 concentrations, the dye molecules start to incorporate into the tetrahedral pores, having a smaller size, which leads to a reduction in the donor-acceptor distances. The above suggestion does not take into account that the donor-acceptor relative orientation can also change with the pore nature. Taking into account the heterogeneity of the system (C153 occupying different sites of the MOF), τ_S should be even shorter than 360 ps observed here, as the whole signal is a combination of the dynamics of those found in small and larger pores. It is remarkably to note that the longest rise time (τ_L ~3.3 ns) of ET from the ligands to C153 is much longer than that of excimer formation (0.65 ns),[37] indicating that the included dye structurally disturbs the interaction between the organic linkers in the MOF network. Moreover, the emission lifetime of the excimers largely decreases (from 13.9 to 6.8 ns) with C153 additions (Figure S3 C, ESI†) demonstrating the disappearance of excimers in favor of produced C153 at S_1 due to ET from the excited monomers.

Scheme 1 gives a summary of the observed dynamics occurring in the C153@Zr-NDC complex in a DE suspension after photoexcitation at the Zr-NDC absorption region. The excited Zr-NDC monomers follow two different routes: 1) They can return to the ground state emitting at 370-420 nm with a lifetime of 2.5 ns (lower than the observed one for Zr-NDC, 3.7 ns) and; 2) they can transfer energy to C153 molecules, which relax to the ground state emitting at 515 nm in 6.8 ns. The ET time depends on the doping, which indicates a clear site-specific dynamics. The red-shift in the emission spectrum together with the increase in the lifetimes indicate that C153 molecules are trapped within the MOF pores. Combining two guests may result in a multicolor emission hybrid material (see section 3.3).

3.2. Nile Red@Zr-NDC Composite

3.2.1. Steady-State UV-Visible Absorption and Emission Spectra

To the above end, we investigated the photoluminescence properties of Zr-NDC when a very well-known fluorescent dye, Nile Red (NR), is allocated into its porous structure. The addition of NR (final concentration ~2.5 x 10^{-5} M) to a Zr-NDC DE suspension and after a subsequent sonication, leads to complexes formation with a loading of 60 % (calculated using the NR absorption spectra before and after its interaction with the MOF). NR molecule is too large (7.6 Å x 13.8 Å) to be included into the tetrahedral cages (pore size = 11 Å) being only possible its allocation into the octahedral ones (pore size = 14 Å) (Scheme S1 in ESI†). The lower loading reflects the guest-host sizes influence in addition to specific and non-specific interactions. The absorption and emission properties of NR@Zr-NDC were investigated (Figure 3). We can distinguish three regions in the absorption spectrum: I) at 320-400 nm, where the absorption corresponds to Zr-NDC; II) 400-550 nm, where NR absorbs in pure DE solution; and III) 550-700 nm, where an unexpected band, red-shifted and with the maximum at 625 nm is recorded. We assign this band to the absorption of the encapsulated or interacting NR molecules with the MOF. Compared to the absorption of the free NR molecules in DE, the interacting ones show a very large bathochromic shift of 125 nm (4000 cm^{-1}), indicating a stronger interaction with the MOF. We suggest that trapped NR molecules are interacting with the -OH groups of the Zr-metal cluster, producing the red-shift of the absorption band. The solvatochromism of NR is very well studied and concludes that H-bonding interactions with the surrounding largely shift the absorption spectrum of NR.[41] The fluorescence spectrum exciting at 335 nm (Zr-NDC absorption region) shows two main emission bands: one located at the blue part (~ 400 nm) which is due to the Zr-NDC and another situated at the

red one (~ 660 nm) which is the emission of the interacting NR. Moreover, there is a small shoulder whose maximum is located at 570 nm, which is similar to that of the emission maximum of NR molecules in DE. Therefore this low intensity band is assigned to the emission of free NR molecules. It is worth to note, the large red shift (90 nm, 2400 cm^{-1}) observed in the emission spectrum of interacting NR molecules when compared to that of free NR ones (from 570 to 660 nm).

Comparable results to those observed here were found by our group when NR is interacting with the hydroxyl groups of the mesoporous material MCM-41.[42] In that report, we observed three different absorption bands having their maximum at 584 and 646 nm due to NR aggregates and at 618 nm owing to monomers. The emission spectra were composed by two bands whose maxima are at 670 (monomers) and 720 nm (J-aggregates). The large red-shift (in ethanol the maxima absorption and emission are at 555 and 630 nm, respectively) was not only due to solvatochromic effect, but also by the strong polarization of the dye molecules interacting with the MCM-41 framework. Both, the maximum absorption and emission of NR/MCM-41 monomers almost coincide with those observed here, so we suggest that NR monomers are strongly interacting with the –OH groups of the Zr-metal cluster, generating a strong polarization of the trapped dye molecules. Note that NR aggregates formation is not possible here due to the MOF pores size. As C153 is less sensitive to the environment (when compared to NR), the emission spectrum of the encapsulated C153 is shifted only by ~30 nm (1250 cm^{-1}) while for NR the shift is 90 nm. The fluorescence quantum yield (φ) of NR@Zr-NDC exciting at 350 nm is $\varphi = 0.24 \pm 0.02$.

Observing the emission of interacting NR molecules when exciting at Zr-NDC region suggests the occurrence of an energy transfer process from MOF to NR. To further investigate this process, we recorded the NR@Zr-NDC excitation spectrum gating at 675 nm (Figure S4, ESI†). At this wavelength, both free and interacting NR molecules emit, but not Zr-NDC. However, in addition to the expected absorption bands of interacting and free NR molecules (region III and II, respectively), the structured absorption band corresponding to Zr-NDC (region I) is clearly detected, confirming the occurrence of an ET from MOF to NR. The inset of Figure 3 exhibits the color of NR@Zr-NDC emission in a DE suspension upon excitation at 365 nm.

3.2.2. Picosecond-Time Resolved Emission Study

To further elucidate the ET process, we examined the ps-photodynamics of NR@ZR-NDC. The inset of Figure 3 displays the fluorescence decays at 425 nm (MOF emission) and

700 nm (trapped NR molecules emission) and upon excitation at 371 nm. Table 3 contains the values of the extracted data from multi-exponential fits upon excitation at 635 and 371 nm, respectively. While the emission decays of NR in a DE solution exhibit a monoexponential behavior with a lifetime of 4.5 ns those of NR@Zr-NDC exciting at 635 nm (absorption region of the interacting NR molecules) were well fitted to a three-exponential function, giving time constants of τ_1= 480 ps, τ_2= 2.8 ns and τ_3= 6.2 ns (Table 3A). This multiexponential behavior reflects an heterogeneity of the surrounding medium, which provokes different photophysics of the interacting NR molecules.

Exciting the Zr-NDC part at 371 nm and according to the steady-state emission spectrum, the analysis of the ps-dynamics were divided following three regions: I) from 425 to 500 nm which is the Zr-NDC emission region; II) at 580 nm, where the emission is mainly due to the free NR molecules and; III) from 675 to 725 nm which is the emission region of the trapped NR molecules. At region I, comparable multiexponential behavior to that observed for Zr-NDC in a DE suspension was found,[37] with lifetimes of τ_1= 650 ps, τ_2= 3.7 ns and τ_3= 9.3 ns (Table 3B). However the lifetime of the excimers is significantly reduced (from 13.9 to 9.3 ns) and the rising component in the excimers formation is quenched from 650 to 150 ps. The quenching in both, the excimers lifetime and the rising component, indicates that now, and contrary to the observed for C153@Zr-NDC, the energy transfer is from the MOF excimers to NR. Region II exhibits a monoexponential behavior giving a lifetime of 5.2 ns which is similar to the obtained for free NR molecules in DE (4.5 ns). Finally, the emission decays in region III show a biexponential behavior with a shorter rising component and a longer decaying one of τ_1= 390 ps and τ_2= 6.2 ns, respectively. Note that now, we do not observe the 2.8 ns component detected when exciting at 635 nm, indicating that the energy is preferentially transferred to some interacting NR molecules giving a lifetime of 6.2 ns. The longer lifetime of these trapped NR molecules compared to that of the free ones (from ~4.5 ns to 6.2 ns) indicates that the formers are located into more restricted media, where the rotation of the diethylamino group of the guest is prevented, hindering the Twisted Intramolecular Charge Transfer (TICT) process which is the main non radiative deactivation pathway.[43] The 390 ps component is assigned to the ET process from MOF to trapped NR molecules. Note that exciting at 371 nm, we do not detect the 480 ps component observed when exciting at 635 nm, which is close in value (but opposite in sign) to that of the rising one. Thus, we suggest that the risetime constant value of 390 ps might be affected by the short component of 480 ps. The large red shift in the emission spectra and the change in the fluorescence lifetime lead us to believe that NR molecules are trapped within the MOF cages. Scheme 2 (pathway A) summarizes the discussion of the observed dynamics and spectral behaviors.

3.3. Nile Red/Coumarin153@Zr-NDC Composite

Aiming to obtain a white light emissive material from a single particle, and using the previous observations, we adjusted the concentrations of NR and C153 included into the porous structure of Zr-NDC DE suspensions. Remarkably, adding both NR and C153 to obtain a final concentration of 5 x 10^{-6} and 3 x 10^{-6} M, respectively, in a 10 mg/10 ml ether ethylic Zr-NDC suspension, we got a white light emissive material.[32] Figure 4 displays the emission spectrum (λ_{exc}= 335 nm) of the NR/C153@Zr-NDC complex in a DE suspension. The inset shows a picture of the cell under UV irradiation and a representation of the CIE coordinates (0.32, 0.34). The observed white light is of a high quality, very near to the ideal one (0.33, 0.33). The emission spectrum shows three well differentiated regions and the global fluorescence quantum yield exciting at 350 nm is φ = 0.33±0.02. The blue band (I) corresponds to the Zr-NDC emission, the green one (II) is of the trapped C153, and the red one (III) is due to the included NR emitting at ~660 nm. There is a clear ET transfer from the excited Zr-NDC to each trapped dye. However to explore whether a cascaded energy transfer (Zr-NDC → C153 → NR) is happening in a single MOF particle, we recorded the emission spectrum exciting at 410 nm (C153 absorption), as well as the excitation spectrum observing at 500 and 675 nm of NR/C153@Zr-NDC in a DE suspension. Figure S5A (ESI†) displays the emission spectrum upon excitation at 410 nm, due to the fluorescence of the trapped C153 without any emission signature of the trapped NR molecules. Thus, the ET does not happen between trapped C513 and NR molecules. This conclusion is supported by the excitation spectrum of NR/C153@Zr-NDC observing at 675 nm (Figure S5B, ESI†), and which does not show any sign of C153 absorption band, exhibiting only the absorption bands corresponding to free and included NR molecules (region III and IV, respectively) and to the Zr-NDC (region I), as we already described. Moreover, the excitation spectrum observing at 500 nm (Figure S5B, ESI†) only displays the absorption band of trapped C153 (region II) together with the Zr-NDC vibrational absorption one (region I). According to these observations, we suggest that the ET process is originated from the MOF to C153 and to NR in a competitive fashion, and there is no ET from trapped C153 to NR, contrary to a previous system in which PVK nanoparticles containing both dyes show a cascade of ET events.[40] A possible explanation of not having the same behavior is that within the MOF, both dyes are located in cavities not allowing adequate orientations or having a long donor-acceptor distance.

3.4. DCM@Zr-NDC Composite: Steady-State Spectra and Dynamics

Behind the goal to get new white light emissive MOF materials, we tried to simplify the hybrid material by allocating into the Zr-NDC porous structure a known laser dye 4-(dicyanomethylene)-2-methyl-6-(4-dimethylaminostyryl)-4H-pyran (DCM). The addition of DCM (final concentration ~1.5 x 10^{-5} M) to a Zr-NDC DE suspension, and the subsequent sonication give a loading of 80 % (calculated using the DCM absorption spectra before and after its interaction with MOF). DCM cannot be allocated into the tetrahedral pores (pore size = 11 Å) due to its large size (10.1 Å x 13.8 Å, Scheme S1, ESI†), being only possible its inclusion into the octahedral ones (pore size = 14 Å). Figure 5 displays the absorption and emission spectra of DCM@Zr-NDC in a DE suspension together with a picture of the cell emitting white light under UV irradiation. The absorption spectrum reproduces those of DCM and Zr-NDC ones, exhibiting a broad absorption band around 450 nm due to DCM, and the characteristics vibrational bands (at ~350 nm) of the Zr-NDC MOF. The fluorescence spectrum exciting at 335 nm (MOF absorption region) presents a dual emission at the blue (Zr-NDC emission) and red (DCM emission) regions. Blue and red emission bands were observed for DCM@stilbene-MOF and DCM@IRMOF-8, where the red-shifted emission (due to DCM dye) origins after an ET process from the MOF.[23] In our case, the observation of white light emission (inset Figure 5) indicates the occurrence of an ET from MOF to DCM. This interpretation is supported by the excitation spectrum (Figure S6A, ESI†). Observing at 625 nm (Zr-NDC does not emit) the spectrum clearly reproduces the vibrational bands corresponding to the Zr-NDC absorption. The CIE coordinates (0.32, 0.31) are shown in Figure S6B (ESI†). Again, the white light emission is of a high quality near to the ideal one (0.33, 0.33). The fluorescence quantum yield of DCM@Zr-NDC exciting at 335 nm is φ = 0.15±0.03.

To explore the ET process, we investigated the photodynamics of DCM@Zr-NDC. The inset of Figure 5 shows the fluorescence decays observing at MOF (425 nm) and at DCM (650 nm) emission regions upon excitation at 371 nm. Tables 4A-B contain the obtained emission lifetimes using multiexponential fits, together with the related parameters upon excitation at 433 and 371 nm, respectively. Exciting at 433 nm (DCM absorption region) the fluorescence decays were well fitted to a three-exponential function, giving time constants of τ_1= 220 ps, τ_2= 790 ps and τ_3= 2.5 ns (Table 4A). The 220-ps component is similar to that obtained for DCM in a DE solution exciting at the same wavelength. Therefore, we assigned τ_1 to the decay of free DCM molecules present in DCM@Zr-NDC suspension. Two more lifetimes components have to be observed. It is well known that excited DCM shows a twisted

intramolecular charge transfer process (TICT) process. Thereby, emission from its local excited (LE) and TICT states were previously observed by trapping it into the mesoporous material, MCM-41.[44] The encapsulation of DCM into MCM-41 leads to a biexponential behavior of its fluorescence decays, giving times of τ_1= 600 ps and τ_2= 1.9 ns,[44] and assigned to the LE and TICT states, respectively. This behavior is similar to the observed here for DCM trapped into the Zr-NDC. Thus, we suggest the 790 ps component is due to the DCM emission of LE state, while that of 2.5 ns corresponds to the emission from the TICT structure.

Exciting the DCM@Zr-NDC suspension at 371 nm (Zr-NDC absorption region) we observed a different behavior (Table 4B). We discuss the results following the spectral regions: Region I from 425 to 500 nm (the emission is mainly due to the MOF) and region II from 525 to 650 nm (corresponding to the fluorescence of trapped DCM molecules). At region I, we observed a three exponential decay behavior, similar to that found for NR@Zr-NDC complexes, giving time constants of τ_1= 650 ps, τ_2= 3.5 ns and τ_3= 9.9 ns. These components have been previously reported and assigned to the excimers formation time (650 ps), and monomers (3.5 ns) and excimers (9.9 ns) emission lifetimes.[37] As for NR@Zr-NDC complexes, the rising component observed at 500 nm (due to excimers formation) and the excimers lifetime are considerably decreased, leading to suggest that the ET process originates from the excimers species to the included DCM molecules. At region II, we observed a decay of 2.5 ns together with a ~520 ps rising component. The former is equal to that obtained when exciting at 433 nm, and therefore it is assigned to the trapped DCM molecules emitting from the TICT state. The 520-ps rising component is due to the ET from Zr-NDC excimers to the included guest. Note that exciting at 371 nm, we do not detect the component assigned to the LE state emission (790 ps) which is close in value (but opposite in sign) to that of the rising one. Thus, we suggest that the time constant assigned to ET process should contain a contribution from the LE emission decay. Scheme 2 (pathway B) summarizes the above discussion, showing the photoprocesses taking place after DCM@Zr-NDC photoexcitation.

4. Conclusion

In this work, we have reported on the spectral and photophysical properties of a Zr-NDC MOF interacting with three laser dyes (C153, NR or DCM). The formed composites (dyes@MOF) show ET processes from MOF to the dyes, resulting in a tunable material emission. In this way, C153@Zr-NDC emits blue and green lights exhibiting two different mean time ET dynamics (~3.3 ns and ~360 ps) which depends on their location into the pores. NR@Zr-NDC composites emit violet-red light through an ET process taking place from the MOF excimers to NR. Importantly, adjusting the concentration of NR and C153 included into the Zr-NDC framework, we obtained a white light emissive material with almost ideal photonic characteristics. On the other hand, DCM@Zr-NDC composite exhibits a white light emission due to an ET process from MOF excimers to included DCM. The fluorescence quantum yields of these composites range from 15 % (DCM@Zr-NDC) to 41 % (C153@Zr-NDC).

Our new results give information on spectral and dynamical behaviors of Zr-NDC MOF interacting with three laser dyes opening the way to application in science and technology like fluorescence sensors and white light emitting diodes. For their future applications, solid-state studies are needed to explore these possibilities.

Acknowledgments

This work was supported by the MINECO through projects MAT2011-25472, Consolider Ingenio 2010 (CSD2009-0050, MULTICAT), PRI-PIBIN-2011-1283 and MAT2014-52085-C2-2-P. We thank Dr. Jacinto Alonso Azcárate for making the X-rays experiments. M.G. thanks the MINECO for the Ph.D. Fellowship.

Supporting Information Available: Scheme S1 contains the molecular structures of the used dyes (C153, NR and DCM). Figure S1 displays the X-rays diffraction patterns of Zr-NDC, C153@Zr-NDC, DCM@Zr-NDC and NR@Zr-NDC. Figure S2 is a representation of the C153/Zr-NDC relative emission intensities versus the concentration of added C153. Figure S3 exhibits the emission decays of (A) Zr-NDC and (B) C153@Zr-NDC in DE suspensions and the variation of the excimers emission lifetime with the amount of added C153. Figure S4 is the excitation spectrum of NR@Zr-NDC in a DE suspension. Figure S5 shows the fluorescence spectrum of NR/C153@Zr-NDC in a DE suspension upon excitation at 410 nm, and the excitation spectra of NR/C153@Zr-NDC in a DE suspension. Figure S6 presents the excitation spectrum of DCM@Zr-NDC in a DE suspension and a representation of the CIE coordinates of DCM@Zr-NDC composite in DE suspension.

References:

1. T. Zhang; W. Lin, Metal-organic frameworks for artificial photosynthesis and photocatalysis. *Chem. Soc. Rev.* 2014**, 43** (16), 5982-5993.
2. Z.-J. Lin; J. Lu; M. Hong; R. Cao, Metal-organic frameworks based on flexible ligands (FL-MOFs): structures and applications. *Chem. Soc. Rev.* 2014**, 43** (16), 5867-5895.
3. V. Stavila; A. A. Talin; M. D. Allendorf, MOF-based electronic and opto-electronic devices. *Chem. Soc. Rev.* 2014**, 43** (16), 5994-6010.
4. P. Falcaro; R. Ricco; C. M. Doherty; K. Liang; A. J. Hill; M. J. Styles, MOF positioning technology and device fabrication. *Chem. Soc. Rev.* 2014**, 43** (16), 5513-5560.
5. Z. Hu; B. J. Deibert; J. Li, Luminescent metal-organic frameworks for chemical sensing and explosive detection. *Chem. Soc. Rev.* 2014**, 43** (16), 5815-5840.
6. C. Zhang; Y. Che; Z. Zhang; X. Yang; L. Zang, Fluorescent nanoscale zinc(ii)-carboxylate coordination polymers for explosive sensing. *Chem. Commun. (Cambridge, U. K.)* 2011**, 47** (8), 2336-2338.
7. H. Xu; F. Liu; Y. Cui; B. Chen; G. Qian, A luminescent nanoscale metal-organic framework for sensing of nitroaromatic explosives. *Chem. Commun. (Cambridge, U. K.)* 2011**, 47** (11), 3153-3155.
8. Y.-S. Xue; Y. He; L. Zhou; F.-J. Chen; Y. Xu; H.-B. Du; X.-Z. You; B. Chen, A photoluminescent microporous metal organic anionic framework for nitroaromatic explosive sensing. *Journal of Materials Chemistry A* 2013**, 1** (14), 4525-4530.
9. C. Zhan; S. Ou; C. Zou; M. Zhao; C.-D. Wu, A Luminescent Mixed-Lanthanide-Organic Framework Sensor for Decoding Different Volatile Organic Molecules. *Anal. Chem.* 2014**, 86** (13), 6648-6653.
10. B. Chen; Y. Yang; F. Zapata; G. Lin; G. Qian; E. B. Lobkovsky, Luminescent Open Metal Sites within a Metal–Organic Framework for Sensing Small Molecules. *Adv. Mater. (Weinheim, Ger.)* 2007**, 19** (13), 1693-1696.
11. W. Liu; T. Jiao; Y. Li; Q. Liu; M. Tan; H. Wang; L. Wang, Lanthanide Coordination Polymers and Their Ag+-Modulated Fluorescence. *J. Am. Chem. Soc.* 2004**, 126** (8), 2280-2281.
12. B. Chen; L. Wang; Y. Xiao; F. R. Fronczek; M. Xue; Y. Cui; G. Qian, A Luminescent Metal–Organic Framework with Lewis Basic Pyridyl Sites for the Sensing of Metal Ions. *Angewandte Chemie International Edition* 2009**, 48** (3), 500-503.
13. Y. Xiao; Y. Cui; Q. Zheng; S. Xiang; G. Qian; B. Chen, A microporous luminescent metal-organic framework for highly selective and sensitive sensing of Cu2+ in aqueous solution. *Chem. Commun. (Cambridge, U. K.)* 2010**, 46** (30), 5503-5505.
14. D. F. Sava; L. E. S. Rohwer; M. A. Rodriguez; T. M. Nenoff, Intrinsic Broad-Band White-Light Emission by a Tuned, Corrugated Metal–Organic Framework. *J. Am. Chem. Soc.* 2012**, 134** (9), 3983-3986.
15. X. Rao; Q. Huang; X. Yang; Y. Cui; Y. Yang; C. Wu; B. Chen; G. Qian, Color tunable and white light emitting Tb3+ and Eu3+ doped lanthanide metal-organic framework materials. *J. Mater. Chem.* 2012**, 22** (7), 3210-3214.
16. Q. Gong; Z. Hu; B. J. Deibert; T. J. Emge; S. J. Teat; D. Banerjee; B. Mussman; N. D. Rudd; J. Li, Solution Processable MOF Yellow Phosphor with Exceptionally High Quantum Efficiency. *J. Am. Chem. Soc.* 2014**, 136** (48), 16724-16727.
17. Z. Hu; G. Huang; W. P. Lustig; F. Wang; H. Wang; S. J. Teat; D. Banerjee; D. Zhang; J. Li, Achieving exceptionally high luminescence quantum efficiency by immobilizing an AIE molecular chromophore into a metal-organic framework. *Chem. Commun. (Cambridge, U. K.)* 2015**, 51** (15), 3045-3048.
18. P. Horcajada; C. Serre; M. Vallet-Regí; M. Sebban; F. Taulelle; G. Férey, Metal–Organic Frameworks as Efficient Materials for Drug Delivery. *Angew. Chem.* 2006**, 118** (36), 6120-6124.

19. M. R. di Nunzio; V. Agostoni; B. Cohen; R. Gref; A. Douhal, A "Ship in a Bottle" Strategy To Load a Hydrophilic Anticancer Drug in Porous Metal Organic Framework Nanoparticles: Efficient Encapsulation, Matrix Stabilization, and Photodelivery. *J. Med. Chem.* 2013**, 57** (2), 411-420.
20. Y. Takashima; V. M. Martínez; S. Furukawa; M. Kondo; S. Shimomura; H. Uehara; M. Nakahama; K. Sugimoto; S. Kitagawa, Molecular decoding using luminescence from an entangled porous framework. *Nature Communications* 2011**, 2** (1).
21. M. C. So; G. P. Wiederrecht; J. E. Mondloch; J. T. Hupp; O. K. Farha, Metal-organic framework materials for light-harvesting and energy transfer. *Chem. Commun. (Cambridge, U. K.)* 2015**, 51** (17), 3501-3510.
22. H. C. Streit; M. Adlung; O. Shekhah; X. Stammer; H. K. Arslan; O. Zybaylo; T. Ladnorg; H. Gliemann; M. Franzreb; C. Wöll; C. Wickleder, Surface-Anchored MOF-Based Photonic Antennae. *ChemPhysChem* 2012**, 13** (11), 2699-2702.
23. D. Yan; Y. Tang; H. Lin; D. Wang, Tunable Two-color Luminescence and Host-guest Energy Transfer of Fluorescent Chromophores Encapsulated in Metal-Organic Frameworks. *Sci. Rep.* 2014**, 4**.
24. M.-J. Dong; M. Zhao; S. Ou; C. Zou; C.-D. Wu, A Luminescent Dye@MOF Platform: Emission Fingerprint Relationships of Volatile Organic Molecules. *Angewandte Chemie International Edition* 2014**, 53** (6), 1575-1579.
25. V. M. Suresh; S. J. George; T. K. Maji, MOF Nano-Vesicles and Toroids: Self-Assembled Porous Soft-Hybrids for Light Harvesting. *Adv. Funct. Mater.* 2013**, 23** (45), 5585-5590.
26. K. Leong; M. E. Foster; B. M. Wong; E. D. Spoerke; D. Van Gough; J. C. Deaton; M. D. Allendorf, Energy and charge transfer by donor-acceptor pairs confined in a metal-organic framework: a spectroscopic and computational investigation. *Journal of Materials Chemistry A* 2014**, 2** (10), 3389-3398.
27. C. Y. Sun; X. L. Wang; X. Zhang; C. Qin; P. Li; Z. M. Su; D. X. Zhu; G. G. Shan; K. Z. Shao; H. Wu; J. Li, Efficient and tunable white-light emission of metal-organic frameworks by iridium-complex encapsulation. *Nature Communications* 2013**, 4**.
28. Dye/metal-organic framework composite material for white light emission and preparation method thereof. CN patent 103740361: 2014.
29. S. Jin; H.-J. Son; O. K. Farha; G. P. Wiederrecht; J. T. Hupp, Energy Transfer from Quantum Dots to Metal–Organic Frameworks for Enhanced Light Harvesting. *J. Am. Chem. Soc.* 2013**, 135** (3), 955-958.
30. J. K. Klosterman; M. Iwamura; T. Tahara; M. Fujita, Energy Transfer in a Mechanically Trapped Exciplex. *J. Am. Chem. Soc.* 2009**, 131** (27), 9478-9479.
31. A. H. Zewail, Chemistry at the Uncertainty Limit. *Angewandte Chemie International Edition* 2001**, 40** (23), 4371-4375.
32. M. Gutiérrez; A. Douhal, White light emitting Zirconium-based MOFs. *EP15382188* 2015.
33. A. Schaate; P. Roy; A. Godt; J. Lippke; F. Waltz; M. Wiebcke; P. Behrens, Modulated Synthesis of Zr-Based Metal–Organic Frameworks: From Nano to Single Crystals. *Chemistry – A European Journal* 2011**, 17** (24), 6643-6651.
34. V. Bon; I. Senkovska; M. S. Weiss; S. Kaskel, Tailoring of network dimensionality and porosity adjustment in Zr- and Hf-based MOFs. *CrystEngComm* 2013**, 15** (45), 9572-9577.
35. J. A. Organero; L. Tormo; A. Douhal, Caging ultrafast proton transfer and twisting motion of 1-hydroxy-2-acetonaphthone. *Chem. Phys. Lett.* 2002**, 363** (3–4), 409-414.
36. W. Zhang; H. Huang; D. Liu; Q. Yang; Y. Xiao; Q. Ma; C. Zhong, A new metal–organic framework with high stability based on zirconium for sensing small molecules. *Microporous Mesoporous Mater.* 2013**, 171** (0), 118-124.

37. M. Gutiérrez; F. Sánchez; A. Douhal, Spectral and Dynamical Properties of a Zr-Based MOF. *submitted to pccp* 2015.
38. T. Kamijo; A. Yamaguchi; S. Suzuki; N. Teramae; T. Itoh; T. Ikeda, Solvation Dynamics of Coumarin 153 in Alcohols Confined in Silica Nanochannels. *The Journal of Physical Chemistry A* 2008**, 112** (46), 11535-11542.
39. M. L. Horng; J. A. Gardecki; A. Papazyan; M. Maroncelli, Subpicosecond Measurements of Polar Solvation Dynamics: Coumarin 153 Revisited. *The Journal of Physical Chemistry* 1995**, 99** (48), 17311-17337.
40. C. Martin; S. Bhattacharyya; A. Patra; A. Douhal, Single and multistep energy transfer processes within doped polymer nanoparticles. *Photochem. Photobiol. Sci.* 2014**, 13** (9), 1241-1252.
41. H. Tajalli; A. G. Gilani; M. S. Zakerhamidi; P. Tajalli, The photophysical properties of Nile red and Nile blue in ordered anisotropic media. *Dyes Pigm.* 2008**, 78** (1), 15-24.
42. C. Martín; P. Piatkowski; B. Cohen; M. Gil; M. T. Navarro; A. Corma; A. Douhal, Ultrafast Dynamics of Nile Red Interacting with Metal Doped Mesoporous Materials. *The Journal of Physical Chemistry C* 2015.
43. P. Hazra; D. Chakrabarty; A. Chakraborty; N. Sarkar, Intramolecular charge transfer and solvation dynamics of Nile Red in the nanocavity of cyclodextrins. *Chem. Phys. Lett.* 2004**, 388** (1–3), 150-157.
44. H. Guo; X. Zhang; M. Aydin; W. Xu; H.-R. Zhu; D. L. Akins, Spectroscopy and dynamics of DCM encapsulated in MCM-41 and Y zeolite mesoporous materials. *J. Mol. Struct.* 2004**, 689** (1–2), 153-158.

Captions of figures and tables

Scheme 1. Proposed mechanisms for photoevents taking place after the photoexcitation of an ether ethylic C153@Zr-NDC ([C153] = $1x10^{-4}$ M) suspension. The ET from the MOF monomers (M*) to C153 precludes the excimers (MM*) formation.

Scheme 2. Proposed mechanisms for the photoprocesses occurring after the photoexcitation of NR@Zr-NDC (path A) and DCM@Zr-NDC (path B) in diethyl ether (DE) suspensions. Note that for these composites, the ET happens from MOF excimers (MM*) to the trapped dyes.

Figure 1. UV-visible (A) absorption and (B) emission spectra of Zr-NDC (black dotted line), C153 (black dashed line) and C153@Zr-NDC (red solid line) in DE suspensions. The inset in figure (A) shows the excitation fluorescence spectrum of C153@Zr-NDC in DE suspension normalized to one at the intensity maximum. The observation wavelength was 625 nm. The pictures inserted in (B) are the samples of Zr-NDC (blue) and C153@Zr-NDC (green) in DE suspensions under UV (365 nm) irradiation.

Figure 2. (A) Change of a three-dimensional fluorescence spectrum of C153@Zr-NDC in a DE suspension with C153 concentration. (B) Emission decays of C153@Zr-NDC showing the variation of the rising component with the concentration of C153. The observation wavelength was 550 nm and the samples were excited at 371 nm. (C) Variation of the rising time value in the emission signal at 550 nm of C153@Zr-NDC composites with the amount of added C153. The inset shows C153 molecules trapped within small- (green molecules) and large-size (red molecule) pores of the MOF.

Figure 3. Normalized to the intensity maximum of absorption (black line) and emission (red line) spectra of NR@Zr-NDC in DE suspension. The excitation wavelength for the emission spectra was 335 nm. The inset exhibits the fluorescence decays of upon excitation at 371 nm and observation as indicated. The picture is the emission of the hybrid material NR@Zr-NDC under UV (365 nm) irradiation.

Figure 4. Normalized to the intensity maximum of emission spectra of NR/C153@Zr-NDC in DE suspension. The excitation wavelength was 335 nm. Region I is the emission of Zr-NDC

while region II and III are the emission of C153 and NR interacting with Zr-NDC, respectively. The inset shows a representation of the CIE coordinates of NR/C153@Zr-NDC/C153 material in DE, and a picture which is the sample containing NR/C153@Zr-NDC in DE under UV (365 nm) irradiation.

Figure 5. Normalized to the intensity maximum of absorption (black line) and emission (red line) spectra of DCM@Zr-NDC in DE suspension. The excitation wavelength for the emission spectra was 335 nm. The inset exhibits the fluorescence decays upon excitation at 371 nm and observation as indicated. The inserted picture shows the emission of DCM@Zr-NDC under UV (365 nm) irradiation.

Table 1. Values of time constants (τ_i) and normalized (to 100) pre-exponential factors (a_i) obtained from a global fit of the emission decays of (A) C153@Zr-NDC and (B) Zr-NDC and C153@Zr-NDC in DE suspensions upon excitation at 433 and 371 nm, respectively. The negative sign for a_i indicates a rising component in the emission signal.

Table 2. Variation in the values corresponding to the shortest time constant (rising signal) of C153@Zr-NDC in DE suspensions at different C153 concentrations. The excitation wavelength was 371 nm while that of observation was 550 nm.

Table 3. Values of time constants (τ_i), normalized (to 100) pre-exponential factors (a_i) and fractional contributions (c_{ii}) obtained from the fit of the emission decays of NR@Zr-NDC in a DE suspension upon excitation at (A) 635 and (B) 371 nm. The negative sign for a_1 indicates a rising component in the emission signal.

Table 4. Values of time constants (τ_i), normalized (to 100) pre-exponential factors (a_i) and fractional contributions (c_i) obtained from the fit of the emission decays of DCM@Zr-NDC in a DE suspension upon excitation at (A) 433 and (B) 371 nm. The negative sign for a_1 indicates a rising component in the emission signal.

Scheme 1.

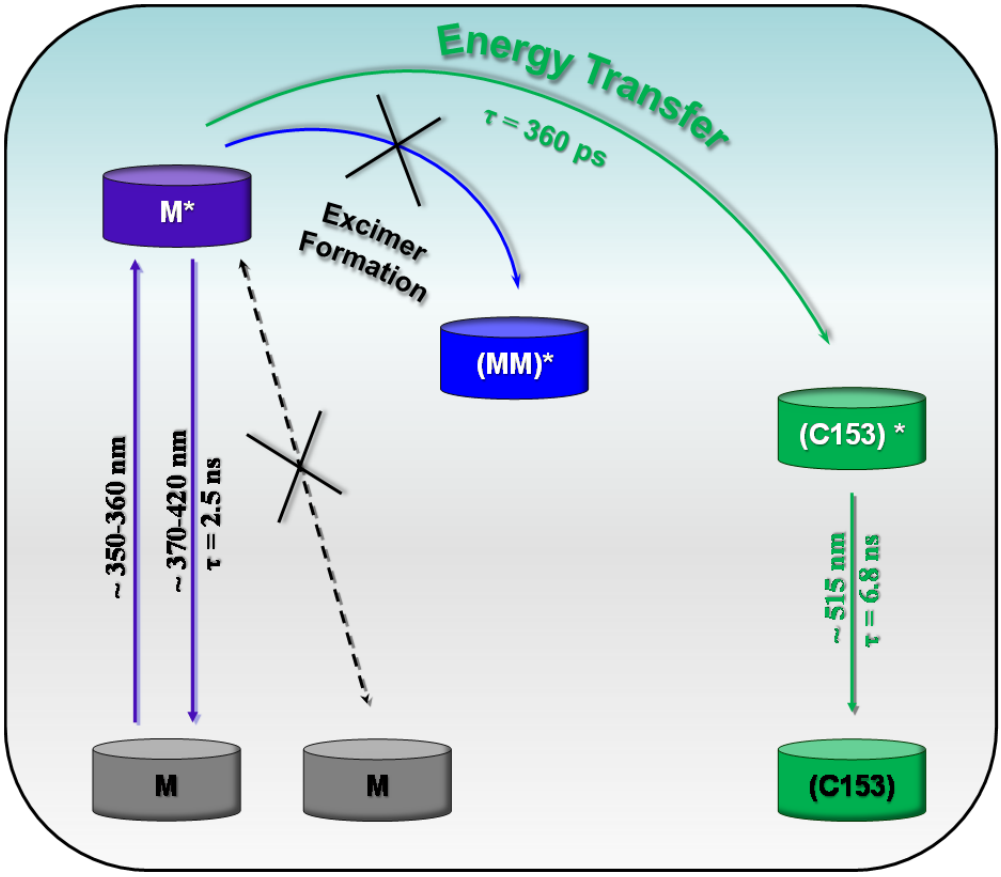

Scheme 2.

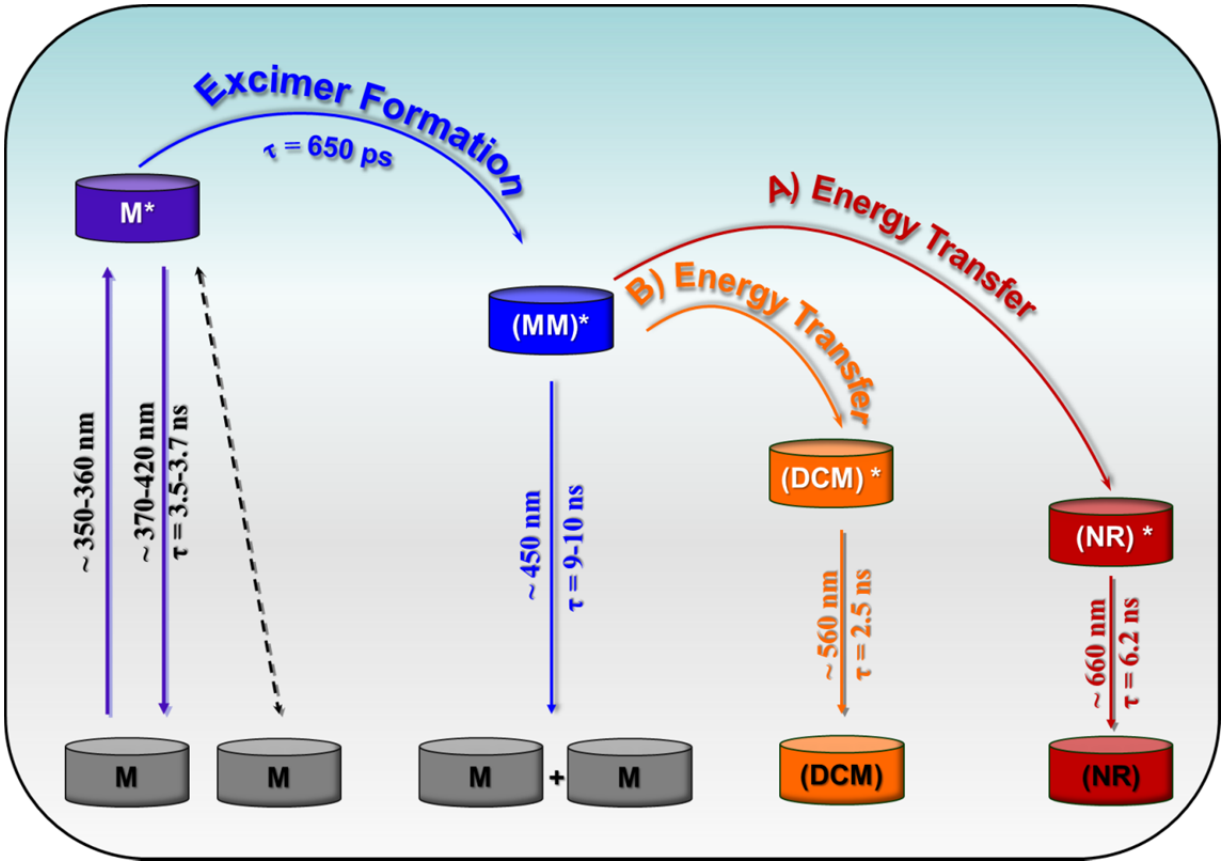

Figure 1.

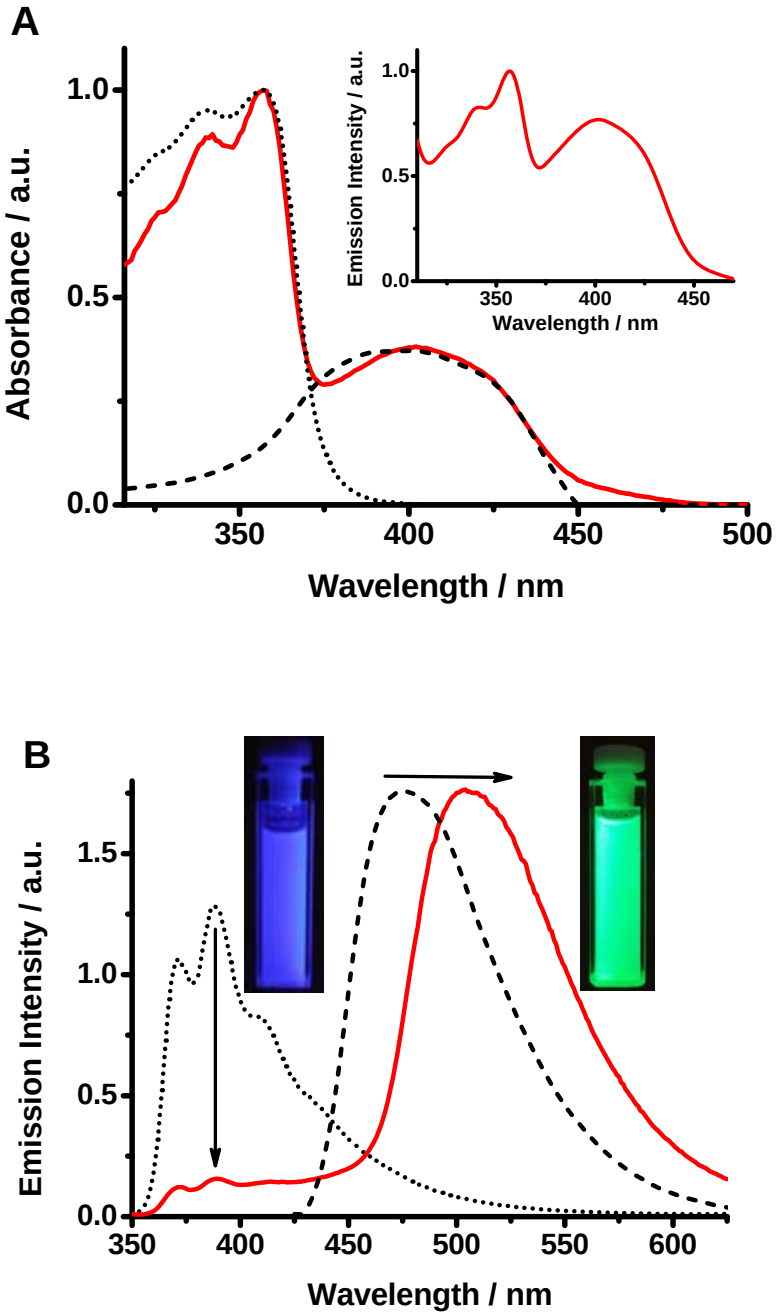

Figure 2.

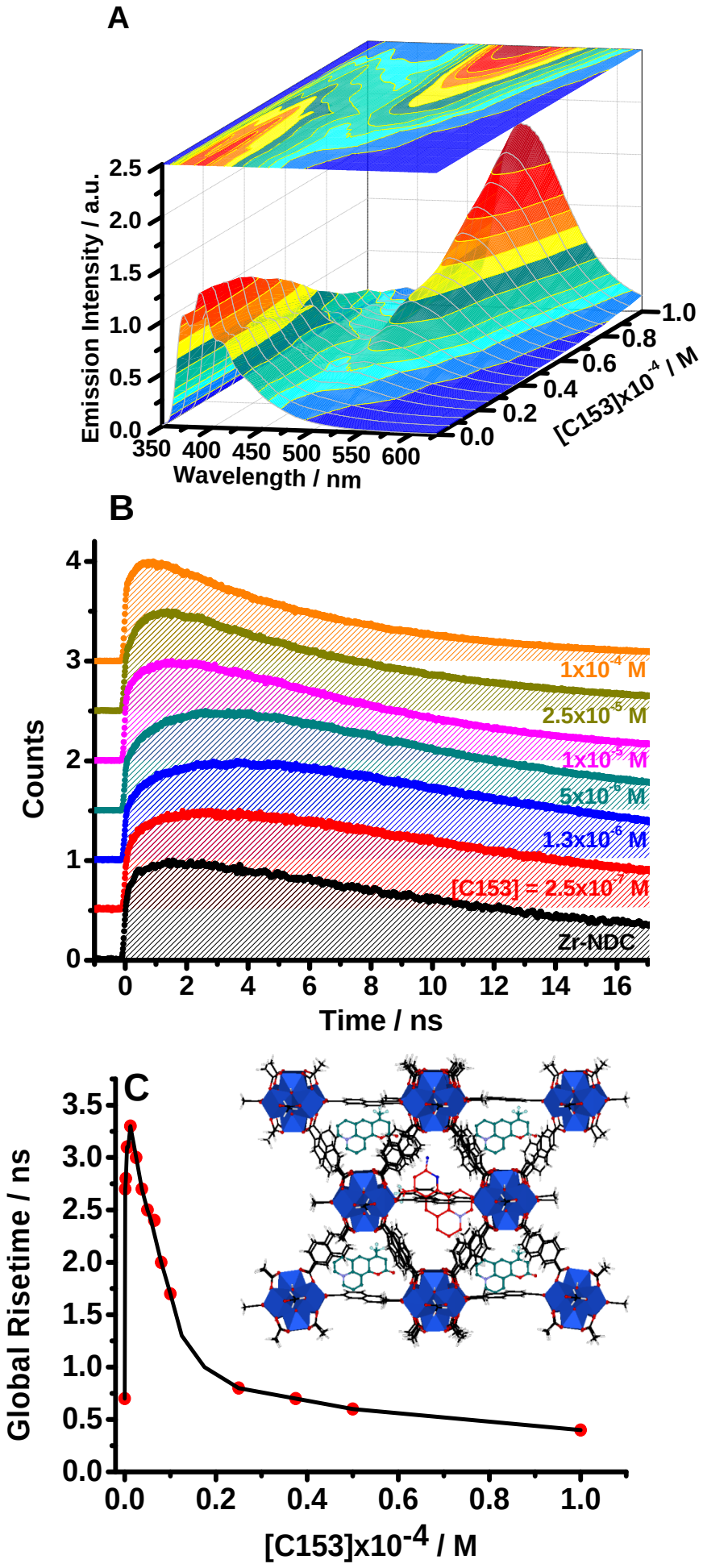

Figure 3.

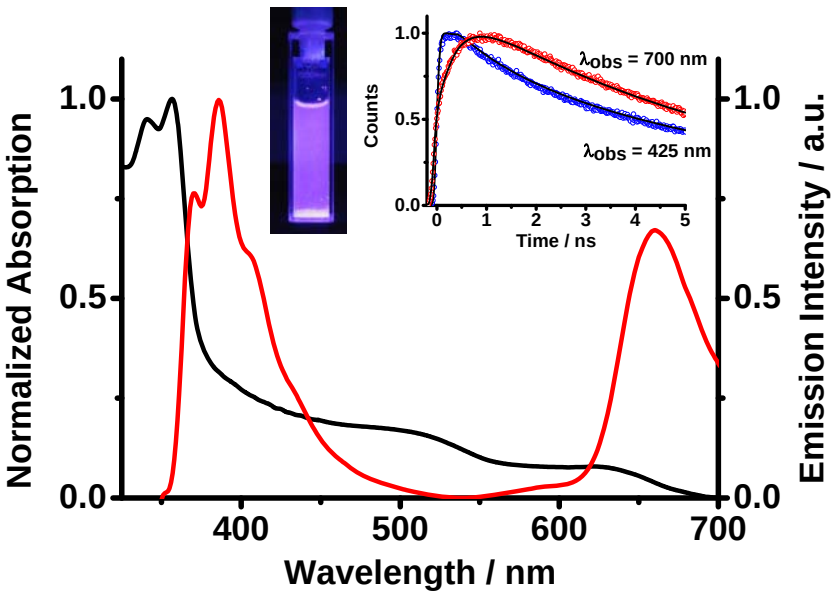

Figure 4.

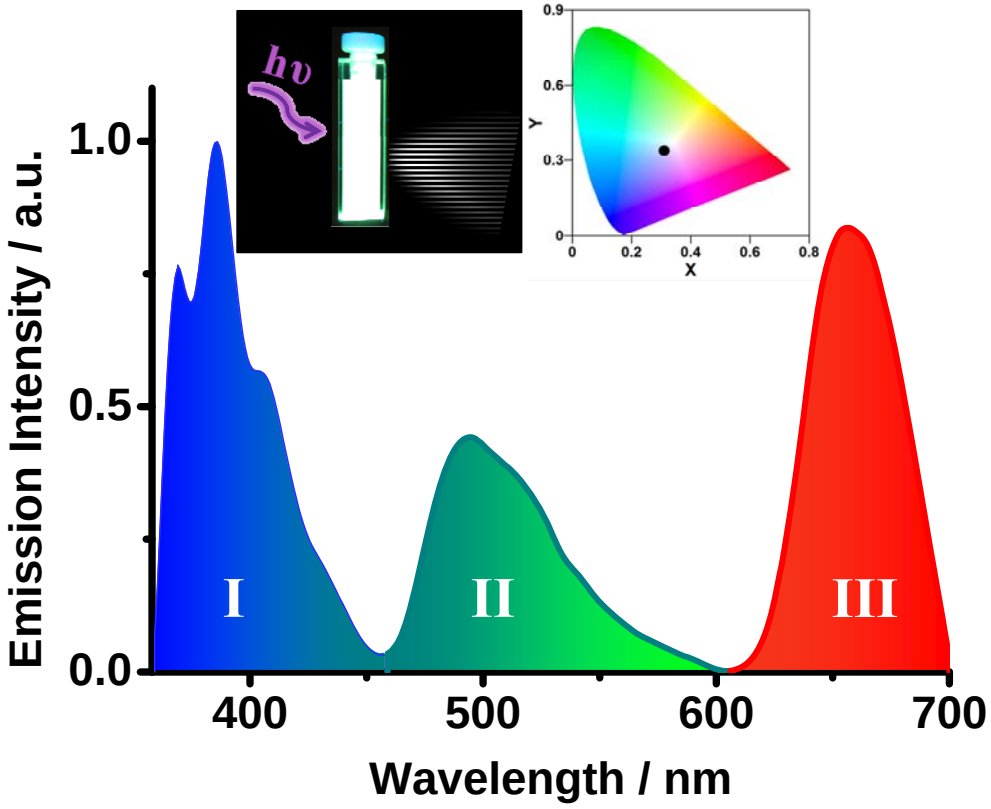

Figure 5.

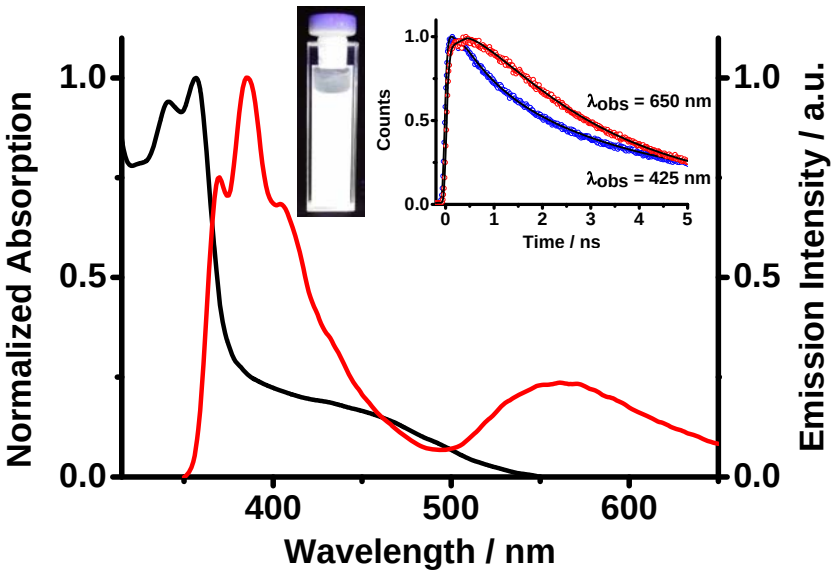

Table 1.

A)

Sample	λ_{Obs}	τ_1 / ns	a_1	c_1	τ_2 / ns	a_2	c_2
C153@Zr-NDC λex = 433 nm	475	1.9	28	9	6.9	72	91
	500	1.9	20	7	6.9	80	93
	525	1.9	15	5	6.9	85	95
	550	1.9	11	3	6.9	89	97
	575	1.9	9	2	6.9	91	98
	600	1.9	8	2	6.9	92	98

B)

Sample	Observation Region	τ_1 / ps	a_1	τ_2 / ns	a_2	τ_3 / ns	a_3
Zr-NDC λex = 371 nm	Blue Part (400-435 nm)	**650**	45	**3.7**	40	**13.9**	15
	Red Part (475-550)	**650**	-100	**3.7**	15	**13.9**	85
C153@Zr-NDC λex = 371 nm	Blue Part (400-435 nm)	**360**	32	**2.5**	48	**6.8**	20
	Red Part (475-600)	**360**	-100			**6.8**	100

Table 2.

[C153]/10^{-6} M	0	0. 1	0. 25	0.5	0. 75	1.25	2.5	3.75	5	6.5	8	10	25	37.5	50	100
τ_1 (risetime) / ns	0.7	2.7	2.8	3.1	3.1	3.3	3	2.7	2.5	2.4	2	1.7	0.8	0.7	0.6	0.36

Table 3.

A)

Sample	λ_{Obs}	τ_1 / ps	a_1	c_1	τ_2 / ns	a_2	c_2	τ_3 / ns	a_3	c_3
NR@Zr-NDC (Diethyl ether) λex = 635 nm	650	480	34	6	2.8	48	50	6.2	18	44
	670	480	19	3	2.8	55	47	6.2	26	50
	700	480	13	2	2.8	58	47	6.2	29	51

B)

Sample	λ_{Obs}	τ_1 / ps	a_1	c_1	τ_2 / ns	a_2	c_2	τ_3 / ns	a_3	c_3
NR@Zr-NDC (Diethyl ether) λex = 371 nm	425	650	23	3	3.7	44	34	9.3	33	63
	450	650	17	2	3.7	33	20	9.3	50	78
	500	150	-100	-100	3.7	26	12	9.3	74	88
	580	-	-	-	-	-	-	5.2	100	100
	675	390	-100	-100	-	-	-	6.2	100	100
	700	390	-100	-100	-	-	-	6.2	100	100
	725	390	-100	-100	-	-	-	6.2	100	100

Table 4.

A)

Sample	λ_{Obs}/nm	τ_1 / ps	a_1	c_1	τ_2 / ps	a_2	c_2	τ_3 / ns	a_3	c_3
DCM@Zr-NDC (Diethyl ether) λex = 433 nm	510	220	72	37	790	24	43	2.5	4	20
	525	220	72	37	790	24	43	2.5	4	20
	550	220	74	38	790	22	40	2.5	4	22
	600	220	73	36	790	22	39	2.5	5	25

B)

Sample	λ_{Obs}/nm	τ_1 / ps	a_1	c_1	τ_2 / ns	a_2	c_2	τ_3 / ns	a_3	c_3
DCM@Zr-NDC (Diethyl ether) λex = 371 nm	425	650	24	4	3.5	52	41	9.9	23	55
	450	650	9	1	3.5	50	29	9.9	41	70
	500	180	-100	-100	3.1	63	33	10.5	37	67
	550	530	-100	-100	2.5	92	82	9.3	8	18
	600	520	-100	-100	2.5	100	100	-	-	-
	650	520	-100	-100	2.5	100	100	-	-	-

Graphical and textual Abstract for the TOC: Nanocomposites of a Zr-Based MOF containing Coumarin 153 and Nile Red show efficient multicolor and white ligth emission.

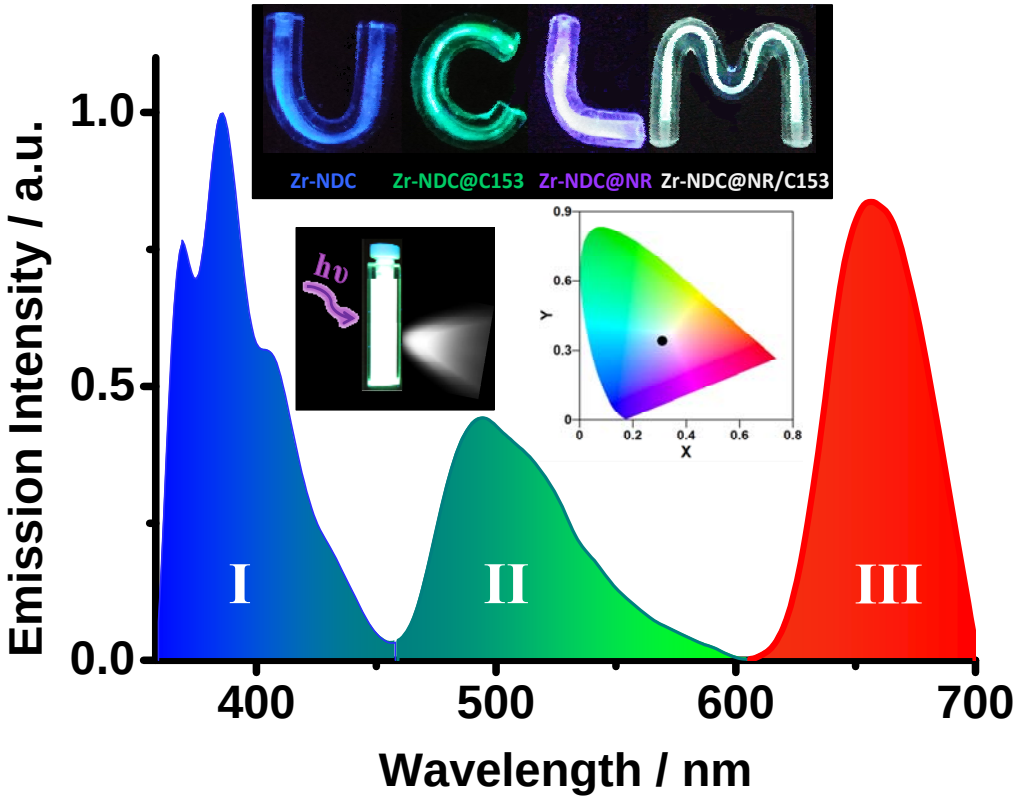

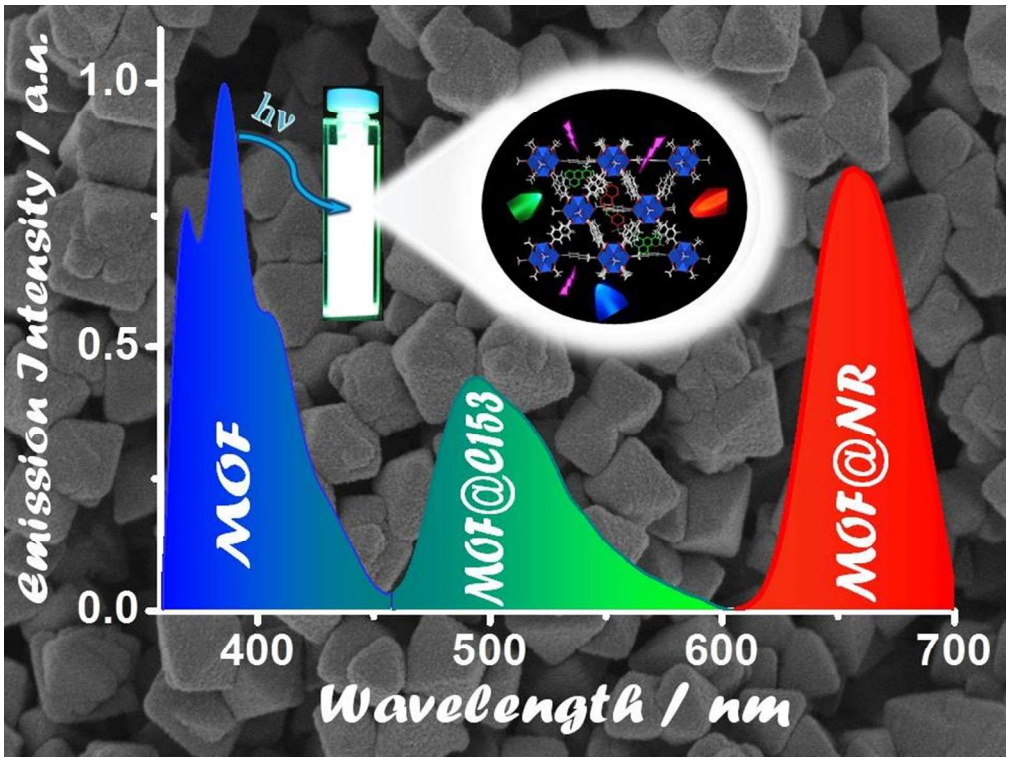

254x190mm (96 x 96 DPI)